12th Int. Conf. on Composite Materials, Paris (July 1999), T. Massard & A. Vautrin (eds.) CD-ROM edition, paper 589.

PREPARATION OF CERAMIC/METAL FOAM LAMINATES USING AN IN SITU FOAMING TECHNIQUE

V. Gergely[1], F. Simancík[2], T. J. Matthams[1] and T. W. Clyne[1]

[1] *Department of Materials Science and Metallurgy, University of Cambridge, Pembroke Street, Cambridge, CB2 3QZ, U.K.*
[2] *Institute of Materials and Machine Mechanics, Slovak Academy of Sciences, Racianska 75, 838 12 Bratislava, Slovakia*

SUMMARY: A study has been carried out of the stability of liquid metallic foams during preparation of laminated ceramic/foamed aluminium composites. The fabrication route involves infiltration of the spaces between ceramic layers with expanding semi-liquid metal foam. Examination of the foam macrostructure revealed that cell coarsening is very sensitive to the foam baking parameters (temperature and time). Theoretical analysis of material redistribution in the liquid foam showed that foam stability can be improved by increasing the melt viscosity. This can be achieved, for example, by incorporation of ceramic particles into the precursor material. However, analysis suggests that the size of particles should be kept reasonably small (~ few μm) because the "life time" of small cells is significantly reduced when the particles are larger.

KEYWORDS: layered structure, laminate fabrication, foamed aluminium, cell coalescence.

INTRODUCTION

Laminated ceramic/metal structures are of interest for engineering components requiring property combinations such as low density with high stiffness, strength, toughness and wear resistance. Very low densities can be achieved by replacing the metal constituent with metallic foam. This type of laminate has been recently produced[1] using a solid-state diffusion bonding technique. An alternative approach involves production of the laminate while the foam is generated. This *in situ* concept offers at least two advantages over conventional solid state diffusion bonding. Firstly, the internal gas generation generates higher interfacial pressure than can be applied during solid-state diffusion bonding and secondly the metal is in a semi-liquid/liquid state, which in general promotes better bonding to the ceramic. On the other hand, liquid foam is inherently unstable and prone to coarsening and degradation. This can happen as a consequence of capillary-driven cell wall thinning, gravitational drainage and “Ostwald ripening”. These processes of material redistribution can lead to cell coarsening and degraded structures.

In the present paper experimental results are presented on cell coarsening in liquid foams during laminate production and measures are identified which promote foam stability.

EXPERIMENTAL PROCEDURES

Processing

Precursor Preparation

Precursor material for foam baking was prepared via a powder metallurgy route. Firstly, commercially pure aluminium powder (<150 μm) and Al alloy powders (to adjust the precursor composition) were blended with about 0.4 wt% of (gas-generating) titanium hydride powder (~5 μm). Secondly, the mixture was cold compacted and hot extruded to form cylindrical bars. Extrusion was carried out below the onset temperature for hydrogen evolution from the hydride. Finally, the extruded bars were cut into suitable lengths.

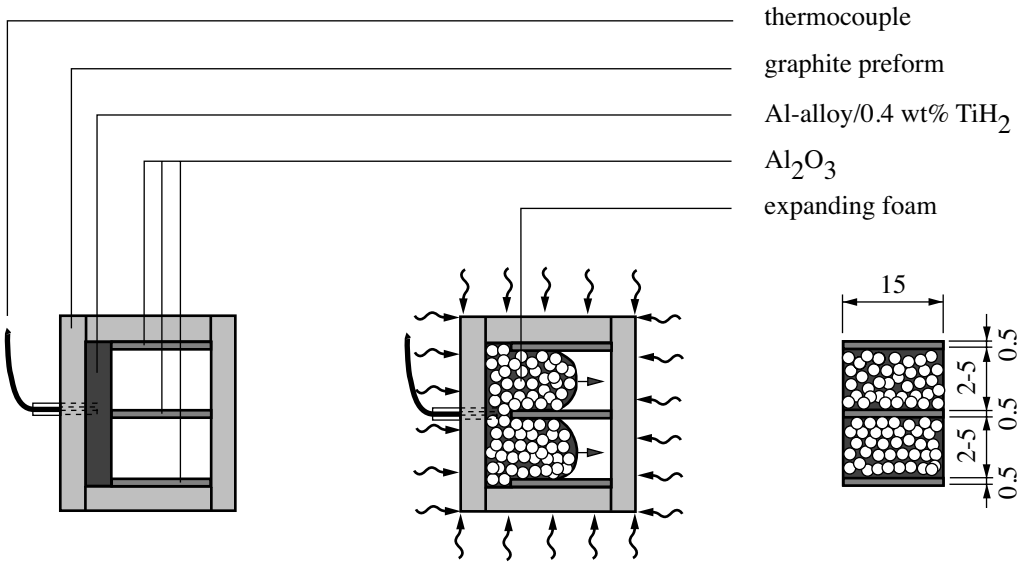

(a) *(b)* *(c)*

Fig. 1: Schematic illustration of the fabrication of laminated ceramic/metal foam. (a) set-up before the foam expansion; (b) heating the composite precursor into a liquid state and foam formation; (c) laminated ceramic/metal foam product.

Laminate Preparation

A schematic depiction of the technique for laminate production is shown in Fig. 1. There are three stages. Firstly, precursor material was placed next to the alumina sheets, which were separated by graphite spacers. Both materials were enclosed in a graphite enclosure. Secondly, this was placed in a furnace and heated until the aluminium alloy became liquid. During this stage the TiH_2 powder decomposed and evolved hydrogen, converting the precursor into an expanding foam which filled the spaces between the ceramic layers. Finally, the foam was allowed to solidify. The free space within the graphite enclosure was about 21.8 cm^3. Processing parameters and specimen codes are listed in Table 1.

Table 1: List of sample codes and processing parameters for laminated alumina/metal foam (Al-1Mg-0.6Si) production.

Sample code	Precursor mass (g)	Baking parameters		
		Heating rate* ($^oC\ min^{-1}$)	Max. temperature (^oC)	Dwell at max. temperature (min)
CF18	20.87	Slow	670	0
CF20	20.97	High	680	~0.18
CF21	21.03	High	660	~0.06
CF22	21.21	Slow	670	~10

* See Figs. 5 (a), (c) and (e)

Foam Characterisation

Image analysis has been carried out on sections of inter-ceramic foam oriented parallel with the alumina layers. The objective of the analysis was to examine the effect of processing parameters (temperature and time of foam baking) on the cell size evolution. The sections were obtained by cutting the foam in the middle of its thickness (5 mm), using electrical discharge machining. Specimens were prepared as follows. Firstly, the surfaces were coated with black paint and open cells were filled with a transparent polyester casting resin (KLEER-SET TYPE FF, MetPrep. Ltd., Coventry, U.K.). Secondly, the surfaces were polished to reveal the cell walls and edges. This procedure ensures that good contrast is achieved between the cell walls/edges and the black background and also eliminates cell wall rupture and smearing during specimen grinding. Finally, a digitised image (800 dpi) of the surface of each specimen was prepared using a scanner. The analysis was carried out using a KS 400 Imaging System, Release 3.0 (Carl Zeiss Vision GmbH, Hallbergmoos, Germany). Cross-sections of cells having a diameter less than 0.35 mm were not included in the analysis. The cell size is represented with a diameter (d) of a circle having an equivalent area to a corresponding cell-section.

MODEL FOR CELL STABILITY

The model is restricted to examination of the tendency for cells to coalesce because of rupture of cell walls as a result of capillary-driven cell wall thinning. Other factors such as inter-bubble gas diffusion and gravitational drainage, which can contribute to foam disintegration, are not incorporated into this version of the model. The foam is assumed to consist of identical pentagonal dodecahedron (PD) cells (see Fig. 2 (a)). The melt is stored in the cell walls and Plateau borders (cell edges) of these polyhedra. As can be seen in Fig. 2 (b), cell walls meet at Plateau borders (PBs), which have strongly curved walls. Because of this curvature (r_{PB}), the pressure in the PB is smaller than in the cell wall (assumed to be planar). This pressure difference represents a driving force for melt to flow from cell walls to PBs, causing the cell wall to rupture when a critical cell wall thickness is reached.

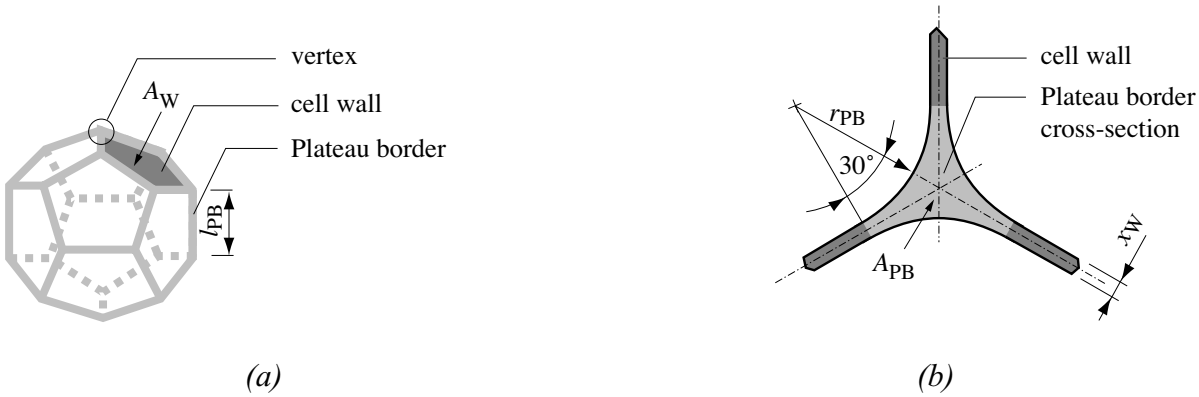

(a) *(b)*

Fig. 2: (a) Isolated pentagonal dodecahedron cell and (b) geometrical definition of the Plateau border cross-section[2],

For a flat cell wall, the pressure in the wall, P_W, is equal to the gas pressure, P_G, in the cell. Using the Laplace-Young equation, the pressure difference, ΔP_C, (capillary pressure) between the pressure in the cell wall and the pressure in the PB, P_{PB}, can be written as

$$\Delta P_C = P_W - P_{PB} = \frac{\gamma}{r_{PB}} \tag{1}$$

where γ is the melt surface tension. The rate of cell wall drainage due to this pressure gradient can be modelled using a Reynolds type equation[3] for flow between two circular parallel disks (assuming immobile wall surfaces)

$$v_W = -\frac{dx_W}{dt} = \frac{2\Delta P_C x_W^3}{3\mu R_W^2} \tag{2}$$

where R_W is the radius of the disk, which has an equivalent area to the pentagonal cell wall (A_W), x_W is the cell wall thickness and μ is the melt viscosity. Substitution of Eqn 1 into Eqn 2 yields

$$v_W = -\frac{dx_W}{dt} = \frac{2\gamma x_W^3}{3\mu R_W^2 r_{PB}} \tag{3}$$

and after rearrangement, the volume change of the cell wall, occurring during a time step dt, can be written as

$$-dV_{W,n} = \frac{2\pi\gamma x_{W,(n-1)}^3}{3\mu r_{PB,(n-1)}} dt \tag{4}$$

The new volume of the PB, $V_{PB,n}$, as result of the material redistribution from the cell walls to the PBs within the time step dt, can be expressed as

$$V_{PB,n} = A_{PB,n} l_{PB} = V_{PB,n-1} + 0.6 dV_{W,n} \tag{5}$$

where $A_{PB,n}$ is a new cross-sectional area of the PB and l_{PB} is the length of the PB (constant for a given cell size). The constant 0.6 in the equation arises because the PD unit cell has six cell walls and ten Plateau borders.

In order to use the above equations for modelling the time dependence of cell wall thinning and rupture, functional relationships are required between all structural parameters of a cellular material (foam porosity, cell size, cell wall area and thickness, cross-sectional area and length of the PB and

the radius of curvature of the PB wall). These relationships have been derived by Gergely and Clyne[4] and are utilised in this work.

The initial state is one with the maximum possible material fraction in the cell walls. This means that the initial structural parameters of the cellular material are calculated for this type of foam. The drainage simulations are divided into a short time steps (dt=0.001 s) and after each step the new geometrical parameters of the foam are calculated. The short time step was necessary in order to capture the drainage behaviour of a low porosity foam (80 %) having a small cell size, lower melt viscosity and relatively high critical cell wall thickness. The process of cell wall thinning is terminated when a critical cell wall thickness is reached. The critical cell wall thickness was assumed to be equal to the diameter of the solid particles present in the melt. Input parameters for the simulations are the unit cell size, D (diameter of a sphere having an equivalent volume to the volume of the PD unit cell), foam porosity, viscosity of the melt, μ, melt surface tension, γ, and the critical cell wall thickness, $x_{W,CR}$.

RESULTS AND DISCUSSION

Examples of laminate structures prepared via the *in situ* foaming technique are shown in Fig. 3. Macrographs of analysed foam structures CF21 (porosity ~72 %), CF20 (porosity ~83 %), CF18 (porosity ~75 %), CF22 (porosity ~77 %), baked under different conditions, are shown in Figs. 4 (a), (b), (c) and (d) respectively. Figs. 5 (a), (b), (c), (d), (e) and (f) shows the thermal profiles of foam baking for CF18, 20, 21 and 22 samples, together with the corresponding cell size distributions in solidified foams. Cell size distributions are expressed as a sum of cell-areas in a corresponding histogram's bins, Sum A(d_{bin}), normalised by the total area of the cells, Sum A(d). The cell size distributions shown in Fig. 5 (b) indicate that, even in case of very short baking times (dwell above the solidus temperature of less than a minute - see Fig. 5 (a)), a change of 20˚C in the maximum baking temperature raised the average cell size appreciably. Figs. 5 (c) and (d) show that the time of foam baking is also important. Longer baking times considerably increase the number of large cells. Cell size distributions for two extreme cases (high heating rate, low maximum temperature and short dwell *vs* low heating rate, high temperature and long dwell) are shown in Fig. 5 (f).

The experimental results suggest that the cell size in metallic foams is very sensitive to the foam baking conditions and a small increase in the baking temperature and/or time significantly accelerates cell coarsening. One way to eliminate rapid cell coarsening, provided the process is controlled by capillary-driven cell wall thinning (and not inter-bubble gas diffusion), is to increase the melt viscosity. This can be achieved, for example, by incorporation of refractory particles into the powder route precursor material. The stabilising effect of solid particles on liquid foams is already utilised in melt route approaches to metallic foam production[5-7]. In general, the size, shape and quantity of ceramic particles are important factors affecting the stability of semi-liquid metallic foams. Typical additions of SiC particles used for stabilisation of semi-liquid Al foams produced by bubbling air through the melt are reported[8] to be: equiaxed particles of mean diameter ~ 1 - 20 μm at concentrations of about 5 - 15 vol%.

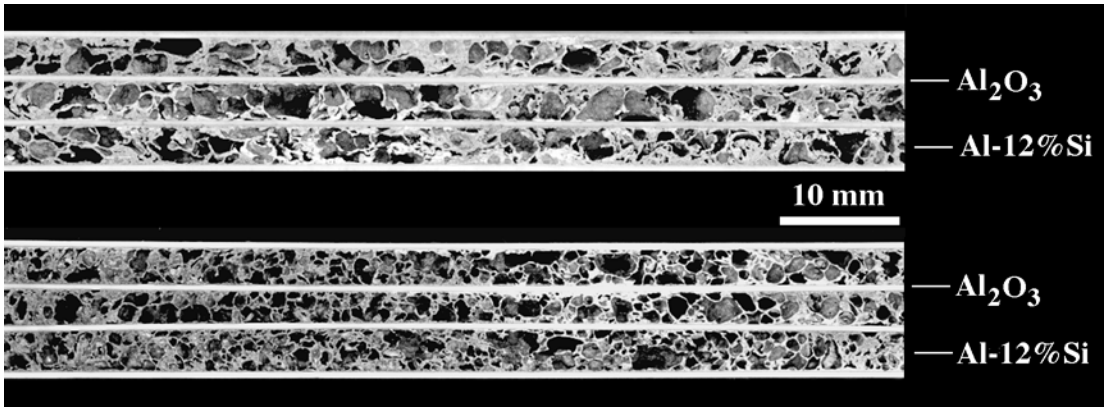

Fig. 3: Sections of laminated alumina/metal foam (Al-12Si) structures.

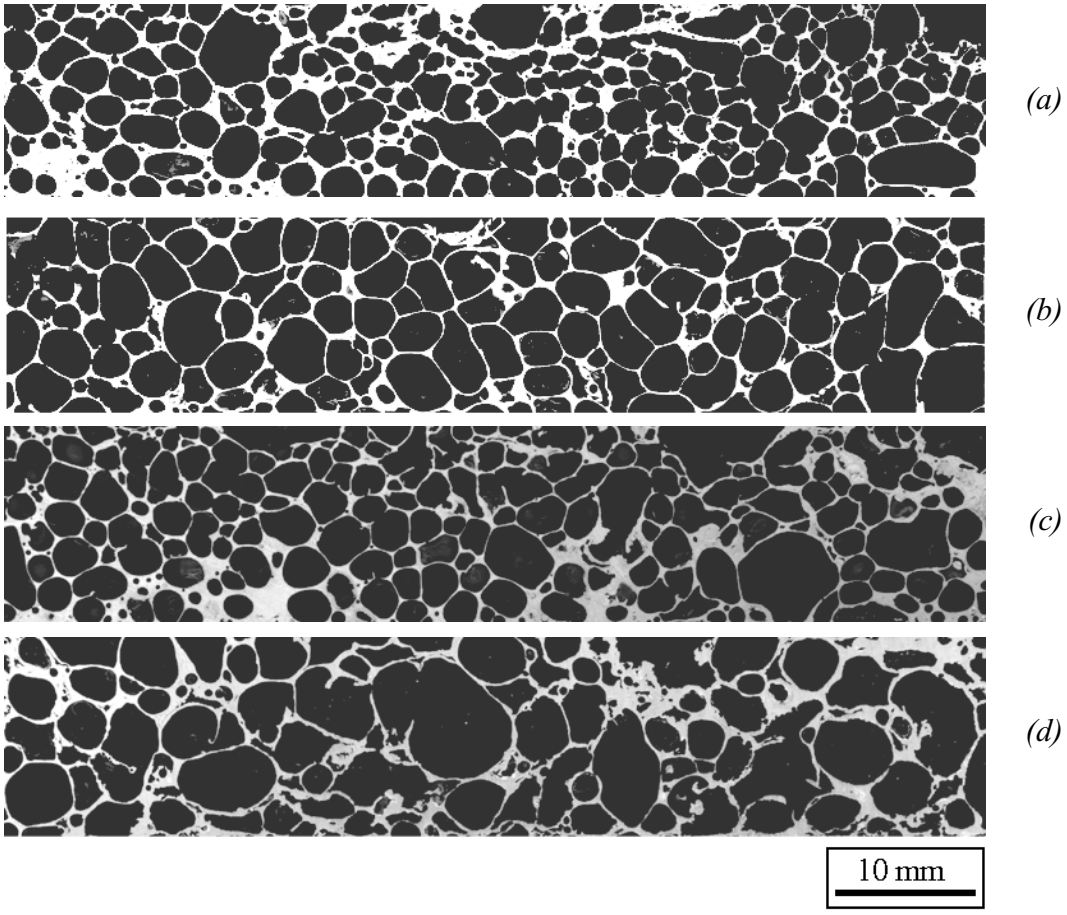

Figs. 4 (a), (b), (c), (d): Macrostructures of inter-laminate Al-1Mg-0.6Si foams (thickness=5 mm) baked under different thermal conditions. (a) sample CF21; (b) sample CF20; (c) sample CF18; (d) sample CF22. Thermal profiles of the foam baking are shown in Figs. 5 (a), (c) and (e).

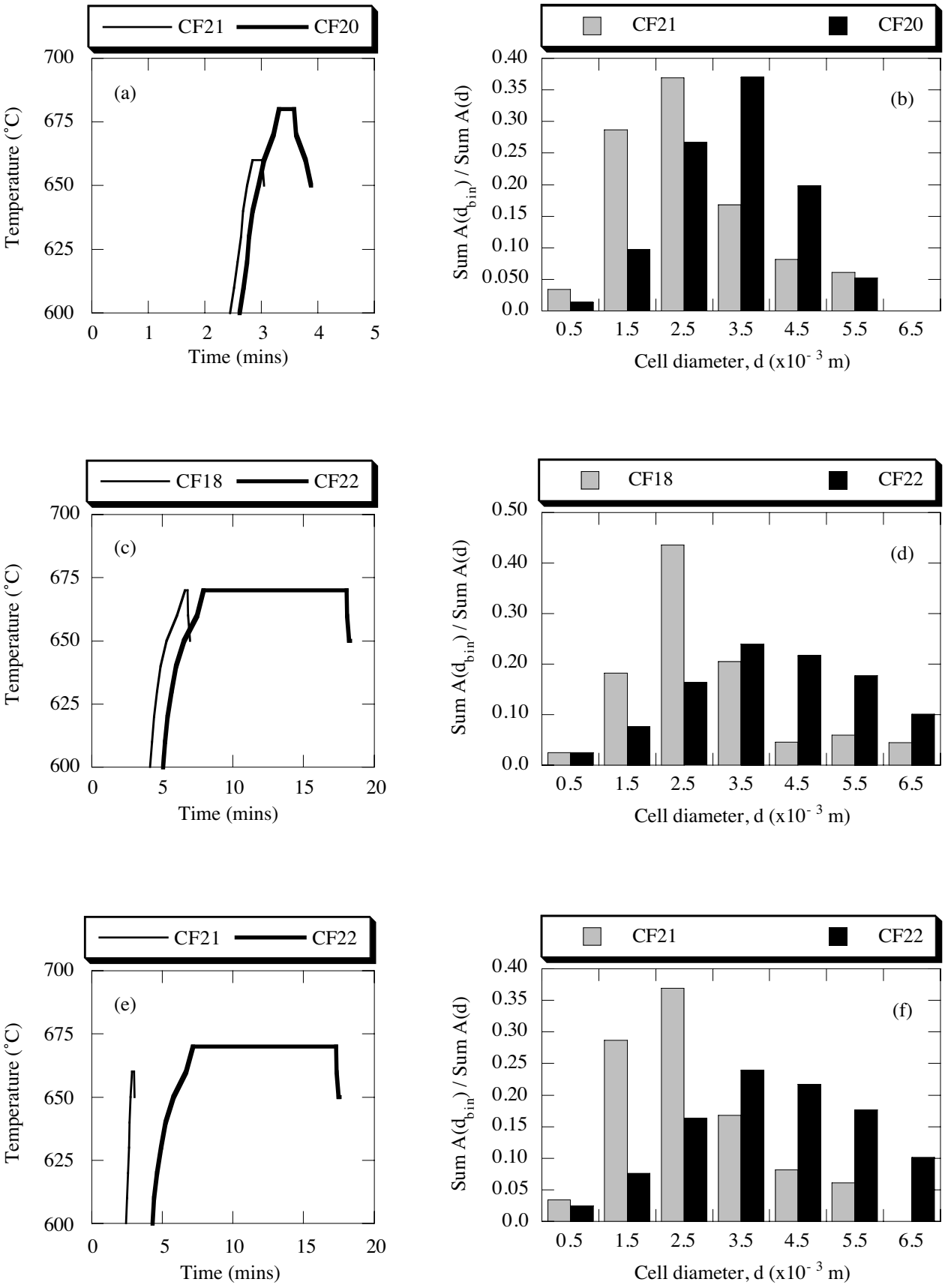

Figs. 5 (a), (b), (c), (d), (e), (f): Plots of thermal histories of the powder route precursor (Al-1Mg-0.6Si/0.4 wt% TiH_2) baking and corresponding cell size, d, distribution in solidified foams (frequency of cell sizes is expressed as a sum of cell areas in a corresponding histogram's bins, Sum A(d_{bin}), normalised with a total area of the cells, Sum A(d)).

Both experimental data for semi-liquid alloys[9] and theoretical predictions[10,11] suggest that viscosity values can vary by several orders of magnitude, depending on the volume fraction of solid particles. The primary objective here was to examine the sensitivity of cell stability to parameters like foam porosity, cell size, viscosity and critical cell wall thickness rather than to make quantitative predictions, so it was acceptable to use order of magnitude estimates for the viscosity.

Fig. 6 (a) shows the predicted dependence of the cell wall rupture time on the unit cell size (D = 1-16 mm), as a function of melt viscosity (μ = 10 and 100 Pa s) and foam porosity level (80 and 95 %). The critical cell wall thickness ($x_{W,CR}$ = 20 μm) and the melt surface tension (γ = 0.855 N m^{-1}) were assumed to be constant in all calculations. Three main features can be identified from the figure. (1) The cell size in foams is controlled by the melt viscosity and by the time available for inter-bubble melt expulsion. (2) The "life time" of smaller cells is significantly shorter in comparison with larger ones. (3) The tendency of cell walls to rupture (a higher cell wall thinning rate) is more pronounced for lower porosity foams (80 %) despite the fact that initial cell wall thickness (the upper bond) is higher than for higher porosity foams (95 %). The reason for this is concerned with development of the foam structural parameters (r_{PB} and R_W), as dictated by the model for the structure of cellular material[4], during cell wall thinning. These parameters are among the factors controlling the cell wall thinning rate (see Eqn 3).

Fig. 6 (b) shows the dependence of the cell wall rupture time on the unit cell size (D = 1-16 mm) for three critical cell wall thicknesses ($x_{W,CR}$=5, 15 and 30 μm). The melt viscosity (μ=10 Pa s), melt surface tension (γ=0.855 N m^{-1}) and foam porosity were constant in these simulations. Results presented on this figure suggest that minimisation of the size of particles present to enhance the melt viscosity significantly improves the stability of semi-liquid foams, provided that the capillary-driven cell wall thinning is the main origin of cell coarsening.

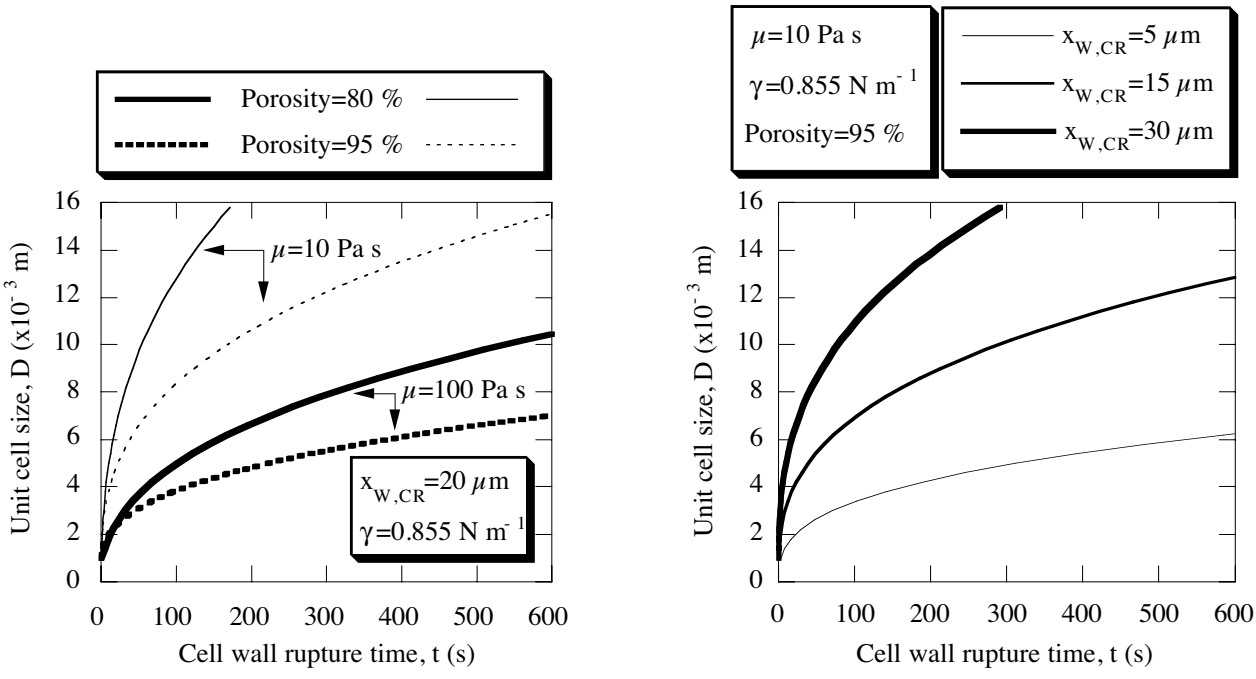

(a) *(b)*

Fig. 6: Plots of the dependence of the cell wall rupture time on the cell size for (a) fixed critical cell wall thickness, $x_{W,CR}$, and two foam porosity and melt viscosity, μ, levels and (b) fixed melt viscosity, μ, and foam porosity and three critical cell wall thicknesses, $x_{W,CR}$.

CONCLUSIONS

An *in situ* foaming technique has been developed for preparation of ceramic/metal foam laminates. The technique is based on infiltration of spaces between ceramic sheets with expanding semi-liquid metal foam. Study of foam cell structures as a function of the processing parameters has shown that cell coarsening is very sensitive to the foam baking conditions (temperature and time).

Theoretical analysis of the stability of semi-liquid foams suggests that enhancement of the melt viscosity is an important method of countering the coarsening and structural degradation which tends to occur even during brief holding periods at high temperature. This can be achieved, for example, by incorporation of refractory particles into the precursor material. However, the size of these particles should be kept small (~ few μm), since larger particles lead to significant acceleration of the cell coarsening process by facilitating cell wall rupture.

ACKNOWLEDGEMENTS

One of the authors (VG) is thankful to the CVCP of UK universities for an Overseas Research Students Award and the Cambridge Overseas Trust for a scholarship. Additional funding was provided by the Department of Engineering through the DARPA/ONR MURI program on Ultralight Metal Structures (No. 00014-1-96-1028).

REFERENCES

1. Markaki, A.E. and Clyne, T.W., "Energy Absorption during Flexural Failure of Layered Metal Foam / Ceramic Composites", *Proceedings of the Twelfth International Conference on Composite Materials*, Massard, T., Ed, Paris, France, 1999.

2. Leonard, R.A. and Lemlich, R., "A Study of Interstitial Liquid Flow in Foam, Part I. Theoretical Model and Application to Foam Fractionation", *A.I.Ch.E. Journal*, Vol. 11, 1965, pp. 18-25.

3. Reynolds, O., "On the Theory of Lubrication and its Application to Mr. Beauchamp Tower's Experiments, including an Experimental Determination of the Viscosity of Olive Oil", *Phil. Trans. Roy. Soc. London*, Vol. 177, 1886, pp. 157-234.

4. Gergely, V. and Clyne, T.W., *Acta Mater.*, 1999 *(in preparation)*.

5. Miyoshi, T., Itoh, M., Akiyama, S. and Kitahara, A., "Aluminum Foam, "Alporas": the Production Process, Properties and Applications", *Proceedings of the Symposium on Porous and Cellular Materials for Structural Applications*, Vol. 521, Schwartz, D. S., Shih, D. S., Evans, A. G. and Wadley, H. N. G., Eds, MRS, San Francisco, California, 1998, pp. 133-137.

6. Wood, J.T., "Production and Applications of Continuosly Cast, Foamed Aluminium", *Proceedings of the Symposium on Metal Foams*, Stanton, Delaware, 1997, Banhart, J. and Eifert, H., Eds, pp. 31-35.

7. Gergely, V. and Clyne, T.W., "A Novel Route to Metallic Foam Production", *Proceedings of the Conference on MetFoam '99*, Bremen, Germany, 1999 *(in press)*.

8. Jin, I., Kenny, L.D. and Sang, H., *Stabilized Metal Foam Body*, in *U.S. Patent 5 112 697*, 1992.

9. Loue´, W.R., Landkron, S. and Kool, W.H., "Rheology of Partly Solidified AlSi7Mg0.3 and the Influence of SiC Additions", *Mater. Sci. Eng.*, Vol. A151, 1992, pp. 255-262.

10. McBirney, A.R. and Murase, T., "Rheological Properties of Magmas", *Ann. Rev. Earth Planet Sci.*, Vol. 12, 1984, pp. 337-57.

11. Veytsman, B., Morrison, J., Scaroni, A. and Painter, P., "Packing and Viscosity of Concentrated Polydisperse Coal-Water Slurries", *Energy Fuels*, Vol. 12, No. , 1998, pp. 1031-1039.